Flexibility and function in HIV-1 protease

Linda K. Nicholson[1], Toshimasa Yamazaki[1], Dennis A. Torchia[1], Stephan Grzesiek[2], Ad Bax[2], Stephen J. Stahl[3], Joshua D. Kaufman[3], Paul T. Wingfield[3], Patrick Y. S. Lam[4], Prabhakar K. Jadhav[4], C. Nicholas Hodge[4], Peter J. Domaille[4] and Chong-Hwan Chang[4]

HIV protease is a homodimeric protein whose activity is essential to viral function. We have investigated the molecular dynamics of the HIV protease, thought to be important for proteinase function, bound to high affinity inhibitors using NMR techniques. Analysis of ^{15}N spin relaxation parameters, of all but 13 backbone amide sites, reveals the presence of significant internal motions of the protein backbone. In particular, the flaps that cover the proteins active site of the protein have terminal loops that undergo large amplitude motions on the ps to ns time scale, while the tips of the flaps undergo a conformational exchange on the μs time scale. This enforces the idea that the flaps of the proteinase are flexible structures that facilitate function by permitting substrate access to and product release from the active site of the enzyme.

[1]Molecular Structural Biology Unit, National Institute of Dental Research, [2]Laboratory of Chemical Physics, National Institute of Diabetes and Digestive and Kidney Diseases, and [3]Protein Expression Laboratory, Office of the Director, National Institutes of Health, Bethesda, Maryland 20892 USA
[4]Department of Chemical and Physical Sciences, The DuPont Merck Pharmaceutical Company, Wilmington, Delaware 19880-0400 USA

The aspartyl proteinase of the HIV-1 virus is a homodimeric enzyme that cleaves the polyprotein products of the *gag* and *pol* viral genes, yielding structural proteins and enzymes that are essential to the life cycle of the virus. Inhibition of this proteinase leads to the production of non-infectious viral particles[1,2]. This enzyme has thus become a primary target for drug design based on numerous X-ray structures of the free proteinase and the proteinase complexed with a variety of inhibitors[3]. Structural differences between the viral and cellular proteinases have been exploited to obtain inhibitors specific for the viral enzyme. One significant structural difference between the viral/cellular proteinases is the presence/absence of a structural water coordinated to the tips of the proteinase's flaps and the inhibitor. The cyclic diol inhibitor, DMP323 (Fig. 1*a*)[4] contains a strategically-placed urea oxygen that mimics the oxygen of the key structural water, thereby excluding the water molecule[4,5] and imparting specificity for the viral proteinase. The linear diol inhibitor, P9941 (Fig. 1*b*)[6] is a less specific inhibitor, because it lacks a urea oxygen, and the structural water is retained in the proteinase/P9941 complex[5]. The higher affinity of the DMP323 inhibitor is ascribed to its design, which preorganizes proteinase-binding substituents on a rigid, seven membered ring.

Structural information obtained from X-ray diffraction studies[3] and molecular dynamics simulations[7,8] have indicated that proteinase flexibility plays a significant role in function. Heteronuclear ^{1}H–^{15}N NMR is a powerful approach for elucidating the motions that occur within the protein backbone, and provides information about the amplitudes and rates of motions of individual bonds. Motions over a wide range of time scales, ranging from ms to ps, can be probed. We have employed ^{15}N NMR relaxation techniques to investigate the flexibility of the proteinase bound to the DMP323 and P9941 inhibitors, in order to gain information about proteinase function and inhibitor binding.

Spin relaxation and molecular motion

Nuclear spin relaxation and molecular motion are closely related[9]. This is because molecular reorientation produces fluctuating magnetic fields that cause transitions between nuclear spin states. In proteins, reorientation of the NH bond axis is the motion responsible for relaxation of the amide ^{15}N spin. This motion is characterized by the spectral density function, $J(\omega)$. Physically, $J(\omega)$ is proportional to the amplitude of the fluctuating magnetic field at the frequency ω, and is directly related to three ^{15}N spin relaxation parameters[9,10]: the ^{15}N longitudinal relaxation time, T_1; the transverse relaxation time, T_2; and the nuclear Overhauser enhancement, NOE. These parameters can be measured for nearly every amide site in isotopically labelled proteins using sensitive ^{1}H detected two-dimensional experiments[10–15].

In order to obtain useful information about protein dynamics from relaxation data one must express the spectral density function in terms of quantities that are related to the amplitudes and correlation times (both overall and internal) of molecular motions. In early studies of protein dynamics, the spectral density function was generated using a specific model for protein internal motion, and the suitability of a particular model was judged by comparing measured relaxation parameters

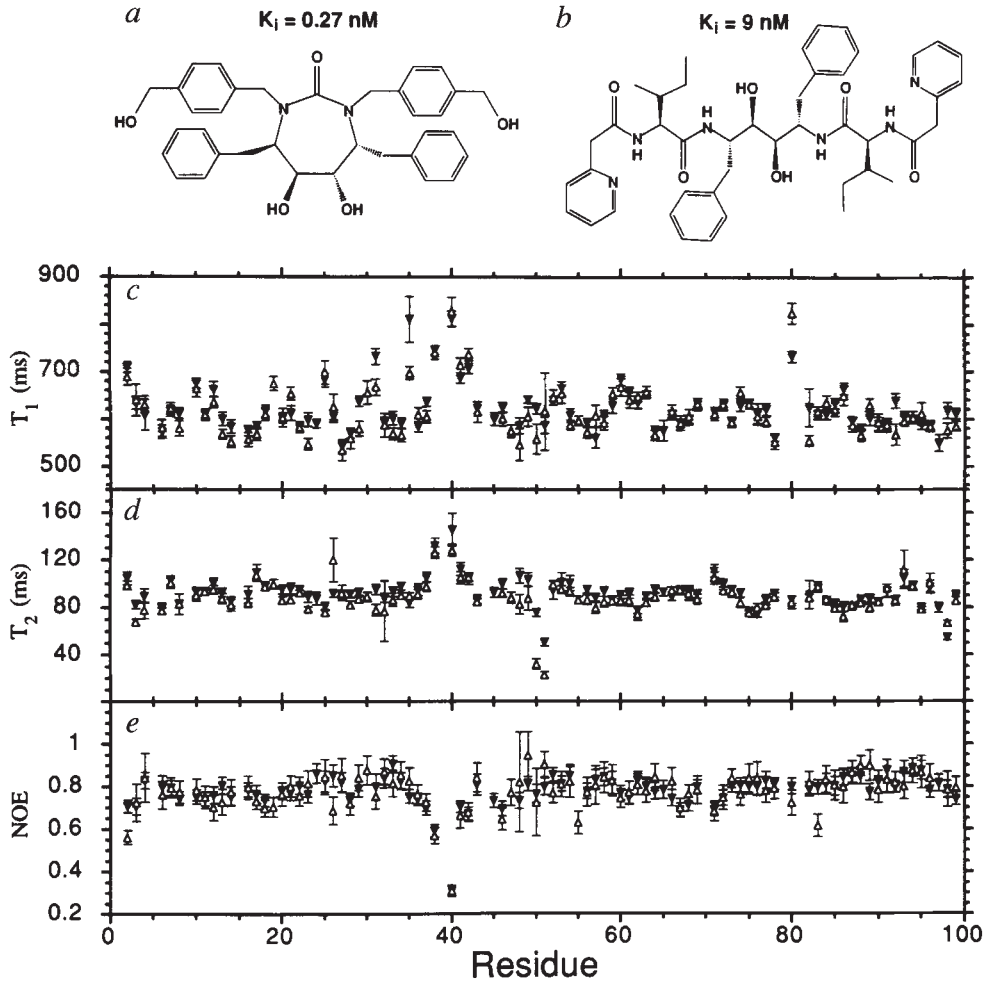

Fig. 1 Inhibitors *a*, DMP323 and *b*, P9941, their respective inhibition constants, K_i, and experimental relaxation parameters *c*, T_1; *d*, T_2; and *e*, NOE values of HIV-1 protease/inhibitor complexes, DMP323 (▼) and P9941 (Δ).

with those calculated using the model. More recently a model-free formalism[16,17] has been developed and is widely used[10,18–24] to extract information about molecular motion from the spectral density function. According to this formalism, when overall motion is isotropic and not correlated with internal motions,

$$J(\omega) = S^2\tau_m/(1 + \omega^2\tau^2) + (1-S^2)\tau/(1 + \omega^2\tau^2) \quad (1)$$

where τ_m is the overall correlation time that characterizes the rigid body rotation of the entire protein, $1/\tau = 1/\tau_m + 1/\tau_e$, τ_e is an effective correlation time characterizing the rapid internal motions (that is, those for which $\tau_e << \tau_m$) of the NH bond, and S is the generalized order parameter. This expression is exact when $(\omega\tau_e)^2 << 1$, which corresponds to $\tau_e < 100$ ps at 500 MHz proton Larmor frequency. The order parameter provides information about the amplitude of the internal motion of the NH bond at each site in the protein, provided that the internal motion is faster than the overall reorientation of the protein, that is $\tau_e << \tau_m$. Although the order parameter is a model independent quantity, it can be readily calculated for any model of NH bond reorientation[16,17]. For example, if the NH bond diffuses in a cone of semi angle θ, S^2 is given by:

$$S^2 = \cos^2\theta^2\,(1 + \cos\theta)^2/4 \quad (2)$$

This equation illustrates that $S^2=1$ in the absence of motion (θ=0°) and $S=0$ when motion is isotropic (θ=180°), results which apply for all types of internal motion. Finally, we note that the equation for $J(\omega)$ has been extended[19] to the case where the internal motion takes place on two fast, but significantly different time scales (that is characterized by correlation times τ_f and τ_s with $\tau_f << \tau_s << \tau_m$).

Chemical exchange

While all three NMR parameters are sensitive to rapid internal motions (on the ps to ns time scale), T_2 is also affected by chemical exchange, on the ms to μs time scale, provided that the chemical exchange affects the ^{15}N chemical shift. In the simplest case, an exchange process involving two states that have equal populations in fast exchange ($\tau_{ex} < T_{CP}/5$, $(\Delta\omega\tau_{ex})^2 << 1$), the exchange contribution, R_{ex}, to $1/T_2$ is given by[25]:

$$R_{ex} = (\Delta\omega/2)^2\,\tau_{ex}((1 - (2T_{ex}/T_{CP})) \quad (3)$$

where τ_{ex} is $2/k$, k is the rate constant for the exchange, Δω is the difference in ^{15}N chemical shifts in the two states (in rad s^{-1}), and T_{CP} is the interval between 180° pulses used in the T_2 pulse sequence[12], ~ 1 ms in the measurements reported here. Because R_{ex} is proportional to $(\Delta\omega)^2$, R_{ex} increases as the square of the external magnetic field, and T_2 measurements at two fields can be used to confirm the presence of conformational exchange. However, such measurements do not yield a value for τ_{ex} unless Δω is known or assumed. It is sometimes possible to determine Δω and τ_{ex} from measurements of $1/T_{1\rho}$, the relaxation rate of spin locked ^{15}N transverse magnetization. For two equally populated sites, the exchange contribution to $1/T_{1\rho}$ is given by[25,26]

$$R_{ex} = (\Delta\omega/2)^2\,\tau_{ex}/(1 + \omega_1^2\tau_{ex}^2) \quad (4)$$

where ω1 is the spin lock field strength. Provided that $\omega_1\tau_{ex}$ ~0.5, measurements of R_{ex} as a function of ω_1 yield both τ_{ex} and Δω.

It is perhaps worth noting that, because Δω is typically ≤ 2 × 10^3, R_{ex} is insignificant unless τ_{ex} is > 10^{-6}. Even when we speak of the fast limit when discussing chemical exchange, therefore, the fast chemical exchange

time scale is several orders of magnitude slower than the time scale of internal motions (τ_e is in the range ns to ps) that affect the order parameter. In other words, the order parameter is only sensitive to motions on a time scale that is much shorter than the overall correlation time of the protein ($\tau_e << \tau_m$). It is not sensitive to motions on the chemical exchange time scale because $\tau_{ex} >> \tau_m$.

Measurements and analyses

The HIV-1 protease contains two identical monomers (1–99/1'–99'). For both complexes residues X and X' have equivalent chemical shifts, demonstrating that the average dimer conformation is symmetric when bound to each symmetric inhibitor. All backbone amide signals have been assigned[5,27] except for Leu 5, and relaxation parameters were obtained for 86 assigned ^{15}N sites in each complex. Data were not obtained for the six proline residues, for six residues in each complex whose signals were poorly resolved, and Leu 5. The measurement and model-free analysis[13,16,17,19,24] of ^{15}N relaxation parameters, T_1, T_2 and NOE (Fig. 1) yielded the overall correlation time, τ_m, as well as the residue specific order parameters, S^2, internal effective correlation times, τ_e, and rates due to chemical exchange, R_{ex}, for each complex (Fig. 2). As expected on the basis of their nearly identical molecular weights, the overall correlation times for the two complexes were found to be essentially the same, 9.2 ns (DMP323) and 9.3 ns (P9941). These correlation times are in accord with overall correlation times reported[14,21,24,28,29] for proteins having a variety of molecular weights.

Even though the K_i values of the two inhibitors differ by 30-fold, the two complexes have nearly identical average order parameters ($<S^2>$= 0.85, DMP323; $<S^2>$=0.87, P9941). In addition the values of S^2 for individual residues in the DMP323 and P9941 complexes are closely correlated (Fig. 2*a*). Omitting Gly 48, the difference between S^2 values for the two complexes has a root-mean-square value of 0.042, in accord with the average standard errors in S^2: 0.031 for each complex. Structural studies have shown that Gly 48 is hydrogen-bonded to the P3 carbonyl group of linear inhibitors closely analogous to P9941 (ref. 3). DMP323 does not contain a P3 site[4], and the Gly 48 NH does not form a hydrogen-bond in the crystal structure of the proteinase/DMP323 complex. The absence of a Gly 48 hydrogen-bond acceptor in the DMP323 inhibitor is consistent with the significantly smaller value of S^2 observed for Gly 48 in the DMP323 complex.

These observations indicate that, with the exception of Gly 48, the flexibility of the proteinase backbone is essentially the same in the two complexes. One possible interpretation of this result is that the NMR order parameters are not sensitive to the differences in interactions between the proteinase and the two different ligands. A more intriguing interpretation is that, in the bound state, the proteinase interacts equally well with each of the two ligands, in spite of their differences in K_i and structure.

Large amplitudes fast motions

Internal motions on the ns–ps time scale result in values of S^2 that are less than unity. While most residues in both complexes have $S^2 > 0.8$ (Fig. 2*a*), indicating a well ordered backbone structure and restricted internal motion, twelve residues in the DMP323 complex (Fig. 3*a*) and nine residues in the P9941 complex have S^2 values of 0.5–0.76. Order parameters in this range correspond to NH bond reorientation of 40°–70° (using the cone model[16,17] to interpret S^2). Most residues executing large amplitude motions are in loops of the proteinase (Fig. 3*a*). Residues Leu 38, Gly 40, Arg 41 and Trp 42 (residue 39 is a proline) form the largest cluster of residues in this class and are located in the loops (Fig. 3*a*) at the end of the flaps that fold over the active site. These four residues also have $S^2 <$ 0.76 in the P9941 complex, and have elevated *B*-factors in the proteinase/DMP323 crystal structure. Crystallographic studies have indicated that flexibility of the flaps allows substrates and inhibitors access to the active site of the proteinase[3]. Furthermore, proteinase activity is diminished by non conservative, amino-acid substitutions at Leu 38

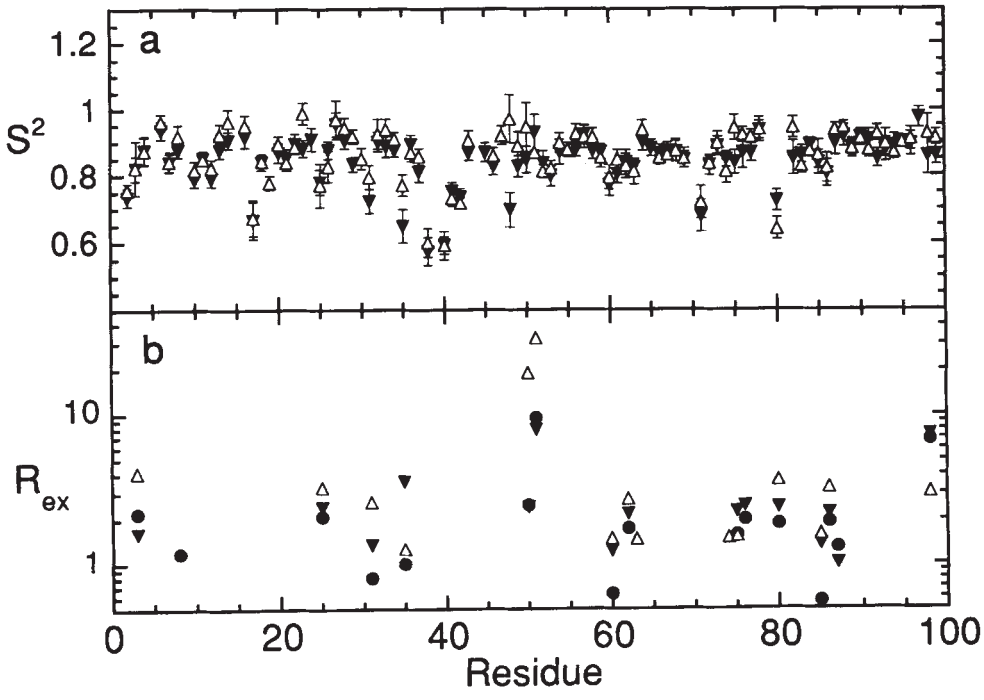

Fig. 2 *a*, Generalized order parameters (S^2) and *b*, the chemical exchange contribution to $1/T_2$ (R_{ex}), plotted as a function of residue number for the two complexes (▼) DMP323 using three relaxation parameters, T_1, T_2 at 500 MHz and NOE at 600 MHz; (●) DMP323 using four relaxation parameters, T_1, T_2 at 500 MHz and T_2, NOE at 600 MHz; and (Δ) P9941 using three relaxation parameters, T_1, T_2 at 500 MHz and NOE at 600 MHz.

and Gly 40, indicating that conformational characteristics of the loop are important for function[30]. Taken together, these results suggest that loop flexibility facilitates substrate binding and product release.

Sites affected by chemical exchange

Our analysis of the relaxation data showed that fifteen residues in the proteinase/DMP323 complex (Fig. 3*b*) were affected by chemical exchange on the ms–μs time scale (Figs 2*b*, 3*b*). Virtually the same residues experience exchange in each of the complexes studied (Fig. 3*b*). Most of these are either involved in inter-monomer contacts or interact with the inhibitor, although a cluster extends across the β-sheet core (residues Asp 60, Ile 62, Val 75 and Leu 76). Based on NMR and X-ray data, it has been proposed[31] that catalytic Asp 25/25' side chains and the diol groups of DMP323 form two hydrogen-bonding networks in dynamic equilibrium. Exchange between these two networks may be responsible for the exchange broadening observed for the amides of Asp 25 and of neighbouring residues Arg 8, Ile 85, Gly 86 and Arg 87 (Fig 3*b*).

Residues at the tips of the flaps (Ile 50 and Gly 51) and in the amino and carboxy termini (Val 3 and Asn 98) are involved in inter-monomer interactions. These residues experience chemical exchange which can be attributed to conformational changes that appear to be related to function. In nearly all proteinase crystal structures, asymmetric βI/βII hydrogen-bonded turn conformations (Fig. 4) are observed at the tips of the flaps[3], however, in the crystal structure of the proteinase/DMP323 complex, symmetric βII/βII non-hydrogen-bonded turn conformations (Fig. 4) are observed. Analysis of a 3D ^{15}N separated NOESY spectrum of the proteinase/DMP323 complex indicates that, in solution, the conformation of the tips of the flaps is not simply a βII turn, but is a mixture of βI and βII turns. Although the asymmetric hydrogen-bonded conformations are indicated by most of the structural data and are consistent with the NMR relaxation and NOESY data, βII/βII symmetric conformation in solution is not excluded. The structural data, taken together with the analysis of the Ile 50/Gly 51 relaxation data, suggest a dynamic model in which the three flap conformations depicted in Fig. 4 undergo exchange.

It should be noted that the conformational transition depicted in Fig. 4 is highly localized, and can be thought of as an approximate 180° flip of the Ile 50/Gly 51 peptide bond. This results in a large change in orientation of the Gly 51 NH bond, which explains the large value of R_{ex} observed for Gly 51 in both the DMP323 and the P9941 complex. In contrast with the orientation of the NH bond of Gly 51, the orientation of the NH bond of Ile 50 is only slightly changed by the proposed flap conformational change. This is a consequence of the position of Ile 50 (residue 2) and Gly 51 (residue 3) in the β-turn and is consistent with X-ray structural data which show that the Ile 50 NH donates a hydrogen bond to an internal water molecule[3] or to the cyclic urea oxygen[4], regardless of whether a βI or βII turn is present. Hydrogen-deuterium exchange experiments show protection factors[32] of at least 100-fold for the Ile 50 NH in both the DMP323 and P9941 complexes, indicating that the Ile 50 NH forms hydrogen bonds in solution. We therefore conclude that the Ile 50 NH bond is not highly flexible, and that the exchange broadening experienced by the Ile 50 amide proton is due to fluctuations in its magnetic environment caused primarily by the large conformational change of neighbouring atoms in the Ile 50/Gly 51 peptide moiety.

An estimate of the correlation time, τ_{ex}, of the flap conformational change was obtained in the following manner. The $T_{1\rho}$ values of the Ile 50 and Gly 51 ^{15}N spins

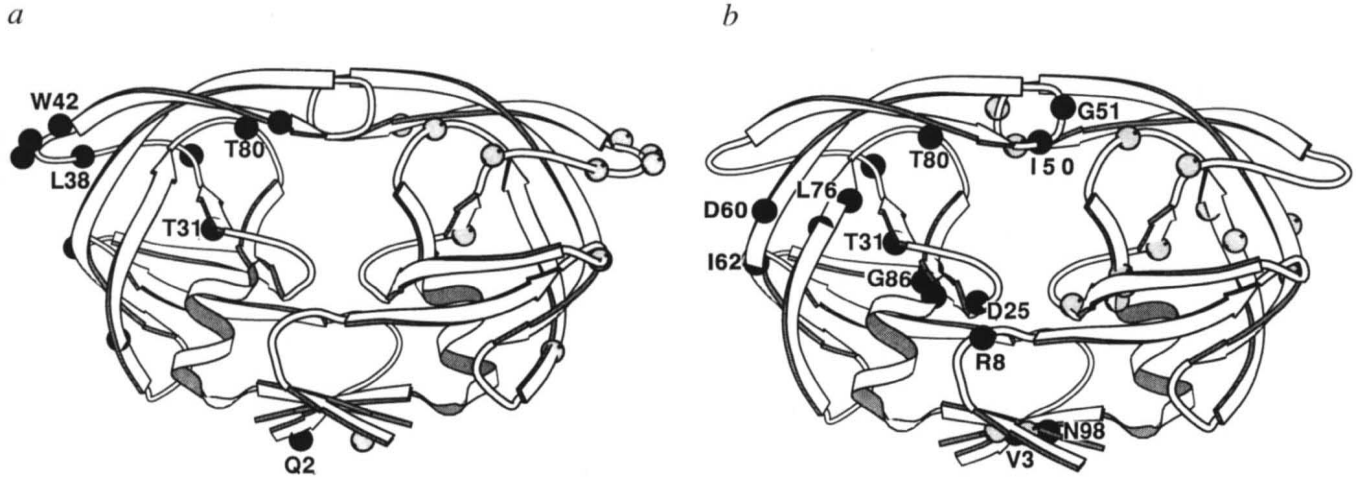

Fig. 3 Proteinase amide sites in the DMP323 complex *a*, undergoing rapid large amplitude motions ($S^2 < 0.76$, three standard deviations less than the average value of S^2): *b*, affected by chemical exchange. Black and stippled spheres identify and distinguish equivalent sites in the two monomer units. The NH bonds of the residues depicted in (*a*) reorient internally on the time scale of ~ 1–100 ps. In the P9941 complex, all sites identified in (*a*) with exception of residues 31, 35 and 48, have $S^2 < 0.76$. The amide sites depicted in (*b*) are affected by chemical exchange processes on the time scale μs–ms. These residues, and essentially the same residues in the P9941 complex, required the inclusion of an exchange term, R_{ex}, to fit the relaxation data. Residues were mapped onto the crystal structure of the proteinase/DMP323 complex[4] using Molscript[42].

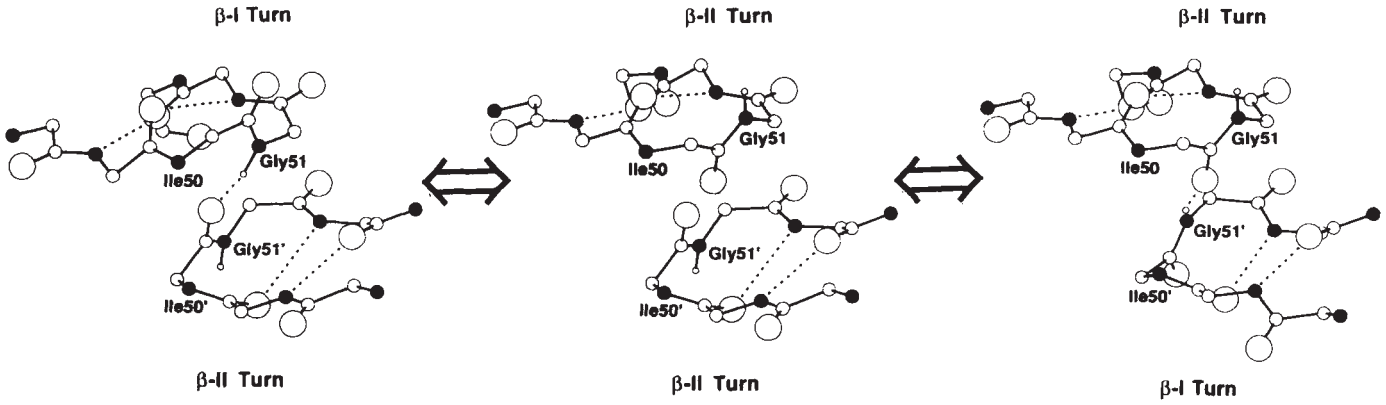

Fig. 4 Proposed model of internal motion at the tips of the proteinase flaps. A conformational switch involving residues Ile (50,50′) and Gly (51,51′). In order to form the hydrogen bond between the Ile 50 carbonyl and the Gly 51' NH group observed in most crystal structures of proteinase/inhibitor complexes[3], the Ile 50/Gly 51 peptide plane in one monomer must be oriented in opposite directions from the Ile 50'/Gly 51' plane in the other monomer. Only the asymmetric conformations will result in the formation of the Ile 50/Gly 51' and Ile 50'/Gly 51 hydrogen bonds. Even though the hydrogen-bonded proteinase conformations are asymmetric, they are isoenergetic and their rapid exchange results in a symmetric NMR spectrum reflecting the dynamic averaging of the homodimer bound to a symmetric inhibitor. The chemical exchange reduces the T_2 values of the Ile 50 and Gly 51 ^{15}N nuclei, demanding the inclusion of a chemical exchange term in the data analysis.

were measured using spin lock fields in the range 1.0–4.5 kHz. At all spin lock fields used, $T_{1\rho}$ was found to be equal (within 10 %) to T_2 for each residue, indicating that chemical exchange is in the fast limit. An upper limit estimate of τ_{ex} was obtained by assuming that the two hydrogen-bonded conformations depicted in Fig. 4 have relative populations of ~ 0.5. Eqs. (3) and (4) show that if $\omega_1/2\pi \leq 4.5$ kHz, $T_{1\rho}$ and T_2 will be nearly equal provided that $\tau_{ex} \leq 10$ μs. Furthermore, eq. (3), combined with the observation that R_{ex} is ≥ 10 for Ile 50 and Gly 51 (Fig. 2) and the estimate that $\Delta\omega \sim 2 \times 10^3$, shows that $\tau_{ex} \sim 10$ μs. We therefore conclude that the flap conformational exchange takes place on the time scale of ~ 10 μs.

Residues Ile 50 and Gly 51 are conserved in retroviral proteinase primary sequences, and non-conservative substitutions of these residues strongly diminish proteinase activity[30], indicating that the structure and dynamics at the tips of the flaps are related to function. We suggest that the various structures formed at the tips of the flaps as observed by crystallography and NMR stabilize the proteinase/substrate complex, yet have the flexibility to facilitate product release following catalysis.

Two additional residues at the dimer interface, Val 3 and its neighbour, Asn 98 (Fig. 3*b*) also experience exchange broadening. All available crystal structures show that these residues have amide protons that are hydrogen bonded and are located in highly ordered β-sheets. ^{15}N and ^{13}C separated NOESY spectra and hydrogen-deuterium exchange protection factors (at least 100-fold for Val 3 and Asn 98 amide hydrogens) confirm that these structural features are also present in solution. In addition, we have seen no evidence for exchange broadening in the ^1H, ^{13}C or ^{15}N signals of the Glu 2 or Asn 98 side chains. It is very unlikely, therefore, that these residues are flexible. The chemical exchange experienced by Val 3 and Asn 98 (and possibly Arg 8) is ascribed to the backbone flexibility of nearby residues Thr 4 and Leu 5, which are in a solvent exposed loop. This statement is supported by the observations that the backbone amide signal of Thr 4 is very weak because it has a very large proton linewidth; and that the amide signal of Leu 5 has not been observed, presumably because it is severely exchange broadened[27]. It is noteworthy that the primary autolysis site in HIV-1 protease is the Leu 5–Trp peptide bond[33], and it has been suggested[33] that the rate of Leu 5–Trp bond cleavage may regulate the activity of the proteinase *in vivo*. If this is the case, the conformational dynamics of residues Thr 4 and Leu 5 could significantly affect the viral life cycle.

Methods

Recombinant HIV-1 protease was expressed in *Escherichia coli* strain BL21(DE3) using a T7 expression system[34]. The protein sequence is that of the HXB2 isolate with an Ala to Cys substitution at position 95. Uniform enrichment with ^{15}N was achieved by growing the bacteria in M9 minimal medium containing $^{15}NH_4Cl$ (Cambridge Isotopes, Cambridge, MA, USA). NMR spectra were recorded on solutions containing the HIV-1 protease/inhibitor complex (0.75mM) in H_2O/D_2O (95%/5%) containing sodium acetate (50 mM, pH 5.2) and dithiothreitol (5 mM). Sample volumes were either 430 μl in Wilmad tubes (Wilmad Glass Company, Buena, NJ, USA) or 220 μl in Shigemi NMR tubes (Shigemi, Inc., Allison Park, PA, USA). NMR tubes were purged with either argon or nitrogen and the Wilmad tubes sealed with a septum cap or by flame, while the Shigemi tubes were tightly wrapped with Teflon tape and parafilm.

T_1 and T_2 values were measured on a Bruker AM 500 spectrometer as described elsewhere[12], with 6–7 relaxation delay points defining each decay curve. T_1 values were determined from two independents sets of relaxation measurements for each complex (data available on request). A numerical fitting approach[22] was used to determine the T_1 values and standard errors (as given by the error bars in Fig. 1) using conjugate gradient minimization and Monte Carlo simulation. T_2 values at 500 MHz were determined from two or three sets of relaxation data sets independently measured for P9941 and DMP323 complexes, respectively. In addition, one set of T_2 values was measured for the DMP323 complex on a Bruker AMX 600 spectrometer (data

not shown). The T_2 values and associated standard errors were determined in the same manner as described for the T_1 data. NOE values were measured on a Bruker AMX 600 spectrometer using inverse detection and a water flip back pulse scheme[35]. Each NOE value was determined from the ratio of signal intensities recorded in the presence or absence of proton saturation. A small correction factor of a few percent was applied to the intensity ratio, to compensate for incomplete magnetization recovery during the recycle delay in the NOE experiment[35]. Standard errors were determined from the r.m.s. noise in the two-dimensional baseplane[35]. The $T_{1\rho}$ data were acquired on a Bruker AM500 spectrometer using continuous ^{15}N spin locking[36] with RF fields of 1.0, 2.0, 3.0 and 4.5 kHz.

To derive τ_m, the ratio T_1/T_2 was calculated for each residue and the average value and standard deviation of the ratio were determined for each complex. Then the relaxation parameters of residues having (a) T_1/T_2 values within one standard deviation of the mean value and (b) NOE values greater than 0.65 were fit assuming a fixed value of τ_m, with model-free parameters S^2 and τ_e allowed to vary until the residual, χ^2,

$$\chi^2 = \Sigma(T_1^{exp} - T_1^c)^2/\sigma_1^2 + (T_2^{exp} - T_2^c)^2/\sigma_2^2 + (NOE^{exp} - NOE^c)^2/\sigma_N^2 \quad \textbf{(5)}$$

was minimized[37]. The equation defines the global χ^2 target function, where the summation extends over the amino-acid residues, the superscripts indicate either experimental or calculated values, and σ_i is the standard error of the parameter, i=1,2,3. The global χ^2 target function was calculated for values of τ_m in the range from 4.0–14.0 ns in steps of 0.1 ns yielding the value of τ_m for which χ^2 was a minimum. With τ_m fixed at this value, residues were selected for which the residue specific values of χ^2 (the χ^2 function calculated for each residue) were less than 4, indicating that they were well fitted by the two parameter model-free formulation. The values of τ_m that minimized the global χ^2 for this set of residues were then determined to be 9.16±0.06 and 9.25±0.06 ns for the DMP323 and P9941 complexes respectively. The uncertainties in the τ_m values represent the 90 % confidence limits in the values of τ_m as determined by the $\Delta\chi^2 \leq 2.71$ criterion[38], and should be regarded as underestimates of the true uncertainties which we estimate to be 2–3 % due to systematic errors (as determined by the reproducibility of relaxation measurements) in the relaxation measurements.

We have assumed that the proteinase reorients isotropically, like a spherical particle. However, the X-ray coordinates[4] show that the protease/cyclic urea inhibitor complex approximates the shape of an oblate ellipsoid of revolution. Including a 3 Å hydration shell[39], the ratio of semi-major axes is calculated to be 1/1.6. Calculations, based on Woessner's equations[40], show that neglect of anisotropic motion for such an oblate ellipsoid introduces r.m.s. errors of 2.3 % in the calculated values of the NMR relaxation parameters. As these errors are smaller than the 2.5–4.5 % r.m.s. errors in the measured relaxation parameters, neglect of anisotropic reorientation will not significantly affect the analysis of the relaxation data. Using overall correlation times of 9.2 and 9.3 ns for the DMP323 and P9941 complexes respectively, the relaxation data for each residue were fitted with the three following formulations of the model-free approach: (1) using two model-free parameters, S^2 and τ_e, where τ_e is an effective correlation time characterizing rapid internal motions of NH bonds on the ps time scale, and S^2 is the generalized order parameter that provides information about the angular amplitude of rapid NH bond reorientation; (2) using S^2, τ_e and a contribution, R_{ex}, (in the equation for $1/T_2$) to account for chemical exchange[10,41]; and (3) using three model-free parameters S_f^2, S_s^2 and τ_s, where $S^2=S_s^2.S_f^2$, and $_s$ and $_f$ refer to rapid internal motions characterized by different time scales[19,24]. The two parameter formulation provided satisfactory fits for all but about twenty residues. Of these, fifteen residues in each complex required inclusion of an exchange contribution, R_{ex}, which is plotted as a function of residue number in Fig. 2*b*. Residues 17, 38, 48 and 71 in the DMP323 complex (17, 38 and 71 in the P9941 complex) required three model-free parameters to fit the relaxation data. Uncertainties in the model-free parameters were determined using a Monte Carlo procedure[14]. Values of τ_e were typically in the range of 1–100 ps, but are not listed individually because their uncertainties were large, usually > 40 %. A particular model-free formulation was considered to provide an adequate fit to the data provided that the residue specific value of χ^2 was less than 6.8. The probability, Q, that a correct model will, by chance, have a residue specific value of χ^2 > 6.8 is 1 %[38]. We prefer accepting a few fitted data sets with low Qs, rather than improving a fit with more parameters that have questionable meaning. In addition, as noted above, our calculated relaxation parameters contain small errors due to anisotropic overall motion and systematic sources. As a consequence of these non-Gaussian sources of error, an acceptable model will have some outlier points with large χ^2 values[38]. Finally, for a few residues having χ^2 > 6.8 it was observed that the error in the (residue specific) relaxation rate was less than the average error in the rate (for all residues). In these cases, the final value of χ^2 was determined using the average error. Because the chemical exchange contribution to T_2 increases as the square of the field strength, a set of T_2 values was also measured at 600 MHz, for the DMP323 complex, and the data analysis was repeated using four sets of relaxation parameters. The same fifteen residues that required an R_{ex} contribution to fit the three relaxation parameters also required an R_{ex} term to best fit the four parameter data, and the values of R_{ex} (at 500 MHz) are plotted in Fig. 2*b*. All fifteen residues had best fit values of χ^2 less than 6.8, except for Gly 35 and Ile 85, suggesting that the motion of these residues must be analyzed using a more complex model or that the errors in their relaxation parameters are underestimated.

Hydrogen exchange rates of backbone amide protons were determined by recording ^1H-^{15}N heteronuclear single quantum spectra as a function of time, ranging from 5 min to 24 hr, after dissolving each complex in D_2O (DMP323 at pD=6.5 and P9941 at pD=5.2, uncorrected meter reading) at 34 °C. Protection factors against exchange were calculated as recently reported[32].

Received 19 January; accepted 7 March 1995.

Acknowledgements
This work was supported by the AIDS targeted Anti-Viral Program of the Office of the Director of the National Institutes of Health.

1. Kohl, N.E. *et al.* Active human immunodeficiency virus protease is required for viral infectivity. *Proc. natn. Acad. Sci. U.S.A.* **85**, 4686–4690 (1988).
2. Seelmeier, S., Schmidt, H., Turk, V. & von der Helm, K. Human immunodeficiency virus has an aspartic-type protease that can be inhibited by pepstatin-A. *Proc. natn. Acad. Sci. U.S.A.* **85**, 6612–6616 (1988).
3. Wlodawer, A. & Erickson, J.W. Structure-based inhibitors of HIV-1 protease. *A. Rev. Biochem.* **62**, 543–585 (1993).
4. Lam, P.Y.-S., *et al.* Rational design of potent, bioavailable, nonpeptide cyclic ureas as HIV protease inhibitors. *Science* **263**, 380–384 (1994).
5. Grzesiek, S. *et al.* NMR evidence for the displacement of a conserved interior water molecule in HIV protease by a non-peptide cyclic urea-based inhibitor. *J. A. chem. Soc.* **116**, 1581–1582 (1994).
6. Jadhav, P.K. & Woemer, F.J. Synthesis of C2-symmetrical HIV-1 protease inhibitors from D-mannitol. *Bioorg. med. Chem. Letts.* **2**, 353 (1992).
7. Harte, W.E. Jr *et al.* Domain communication in the dynamics structure of human immunodeficiency virus-1 protease. *Proc. natn. Acad. Sci. U.S.A.* **87**, 8864–8868 (1990).
8. Venable, R.M., Brooks, B.R. & Carson, F.W. Theoretical studies of relaxation of a monomeric subunit of HIV-1 protease in water using molecular-dynamics. *Proteins Struct. Funct. Genet.* **15**, 374–384 (1993).
9. Abragam, A. *The Principles of Nuclear Magnetism* (Oxford University Press, Oxford, U.K.; 1961).
10. Kay, L.E., Torchia, D.A. & Bax, A. Backbone dynamics of proteins as studied by ^{15}N inverse detected heteronuclear NMR spectroscopy: application to staphylococcal nuclease. *Biochemistry* **28**, 8972–8979 (1989).
11. Boyd, J., Hommel, U. & Campbell, I.D. Influence of cross-correlation between dipolar and anisotropic chemical shift relaxation mechanism upon longitudinal relaxation rates of ^{15}N in macromolecules. *J. chem. Phys.* **175**, 477–482 (1990).
12. Kay, L.E., Nicholson, L.K., Delaglio, F., Bax, A. & Torchia, D.A. Pulse sequences for removal of the effects of cross correlation between dipolar and chemical-shift anisotropy relaxation mechanisms on the measurement of heteronuclear T_1 and T_2 values in proteins. *J. magn. Reson.* **97**, 359–375 (1992).
13. Palmer, A.G., Skelton, N.J., Chazin, W.J., Wright, P.E. & Rance, M. Suppression of the effects of cross-correlation between dipolar and anisotropic chemical shift relaxation mechanisms in the measurement of spin-spin relaxation rates. *Molec. Phys.* **75**, 699–711 (1992).
14. Torchia, D.A., Nicholson, L.K., Cole, H.B.R. & Kay, L.E. Heteronuclear NMR studies of the molecular dynamics of staphylococcal nuclease, in *NMR of Proteins* (eds Clore, G.M. & Gronenborn, A.M.) 190–219 (Macmillan, London; 1993).
15. Wagner, G., Hyberts, S. & Peng, J.W. Study of Protein Dynamics by NMR, in *NMR of Proteins* (eds Clore, G.M. & Gronenborn, A.M.) 220–257 (Macmillan, London; 1993).
16. Lipari, G. & Szabo, A. Model-free approach to the interpretation of nuclear magnetic resonance relaxation in macromolecules. 1. Theory and range of validity. *J. Am. chem. Soc.* **104**, 4546–4559 (1982).
17. Lipari, G. & Szabo, A. Model-free approach to the interpretation of nuclear magnetic resonance relaxation in macromolecules. 2. Analysis of experimental results. *J. Am. chem. Soc.* **104**, 4559–4570 (1982).
18. Dellwo, M.J. & Wand, A.J. Model-independent and model-dependent analysis of the global and internal dynamics of cyclosporin A. *J. Am. chem. Soc.* **111**, 4571–4578 (1989).
19. Clore, G.M. *et al.* Deviation from the simple two-parameter model-free approach to the interpretation of nitrogen-15 nuclear magnetic relaxation of proteins. *J. Am. chem. Soc.* **112**, 4989–4991 (1990).
20. Barbato, G., Ikura, M., Kay, L.E., Pastor, R. & Bax, A. Backbone dynamics of calmodulin studied by ^{15}N relaxation using inverse detected two-dimensional NMR spectroscopy: the central helix is flexible. *Biochemistry* **31**, 5269–5278 (1992).
21. Kordel, J., Skelton, N.J., Akke, M., Palmer, A.G. & Chazin, W.J. Backbone dynamics of calcium-loaded calbindin D9k studies by two-dimensional proton detected ^{15}N NMR spectroscopy. *Biochemistry* **31**, 4856–4559 (1992).
22. Nicholson, L.K. *et al.* Dynamics of methyl groups in proteins as studied by proton-detected ^{13}C NMR spectroscopy. Application to the leucine residues of Staphylococcal Nuclease. *Biochemistry* **31**, 5253–5263 (1992).
23. Constantine, K.L. *et al.* Relaxation study of the backbone dynamics of human profilin by two-dimensional ^{1}H-^{15}N NMR. *FEBS Letts* **336**, 457–461 (1993).
24. Farrow, N.A. *et al.* Backbone dynamics of a free and a phosphopeptide-complexed Src homology 2 domain studied by ^{15}N NMR relaxation. *Biochemistry* **33**, 5984–6003 (1994).
25. Farrar, T.C. & Becker, E.D. *Pulse and Fourier Transform NMR* 1–115 (Academic Press, New York, 1971).
26. Szyperski, T., Luginbuhl, P., Otting, G., Guntert, P. & Wuethrich, K. protein dynamics studied by rotating frame 15N spin relaxation times. *J. Biomol. NMR* **3**, 151–164 (1993).
27. Yamazaki, T. *et al.* Secondary structure and signal assignments of human-immunodeficiency-virus-1 protease complexed to a novel, structure-based inhibitor. *Eur. J. Biochem.* **219**, 707–712 (1994).
28. Clore, G.M., Driscoll, P.C., Wingfield, P.T. & Gronenborn, A. Analysis of the backbone dynamics of interleukin-1β using two-dimensional inverse detected heteronuclear ^{15}N-^{1}H NMR spectroscopy. *Biochemistry* **29**, 7387–7401 (1990).
29. Stone, M.J. *et al.* The backbone dynamics of the *Bacillus subtilis* glucose permease IIA domain determined from *15*N NMR relaxation measurements. *Biochemistry* **31**, 4393–4406 (1992).
30. Loeb, D.D. *et al.* Complete mutagenesis of the HIV-1 Protease. *Nature* **340**, 397–400 (1989).
31. Yamazaki, T. *et al.* NMR and X-ray evidence that the HIV protease catalytic aspartyl groups are protonated in the complex formed by the protease and a non-peptide cyclic urea-based inhibitor. *J. Am. chem. Soc.* **116**, 1994 (1994).
32. Bai, Y., Milne, J.S., Mayne, L. & Englander, S.W. Primary structure effects on peptide group hydrogen exchange. *Prot., Struct. Funct. Genet.* **17**, 75–86 (1993).
33. Rose, J.R., Salto, R. & Craik, C.S. Regulation of autoproteolysis of the HIV-1 and HIV-2 proteases with engineered amino acid substitutions. *J. biol. Chem.* **268**, 11939–11945 (1993).
34. Cheng, Y.-S.E. *et al.* High-level synthsis of recombinant HIV-1 protease and the recovery of active enzyme from inclusion bodies. *Gene* **87**, 243–248 (1990).
35. Grzesiek, S. & Bax, A. The importance of not saturating H_2O in protein NMR. application to sensitivity enhancement and NOE measurements. *J. Am. chem. Soc.* **115**, 12593–12594 (1993).
36. Peng, J.W., Thanabal, V. & Wagner, G. 2D heteronuclear NMR measurements of spin-lattice relaxation times in the rotating frame of X nuclei in heteronuclear HX spin systems. *J. magn. Reson.* **95**, 421–427 (1991).
37. Palmer, A.G., Wright, P.E. & Rance, M. Measurement of relaxation time constants for methyl groups by proton-detected heteronuclear NMR spectroscopy. *Chem. Phys. Letts.* **185**, 41–46 (1991).
38. Press, W.H., Flannery, B.P., Teukolsky, S.A. & Vetterling, W.T. *Numerical Recipes in C* (Cambridge University Press, Cambridge, U.K., 1988).
39. Venable, R.M. & Pastor, R.W. Frictional models for stochastic simulations of proteins. *Biopolymers* **27**, 1001–1014 (1988).
40. Woessner, D.E. Nuclear spin relaxation in ellipsoids undergoing rotational brownian motion. *J. chem. Phys.* **37**, 647–654 (1962).
41. Palmer, A.G., Rance, M. & Wright, P.E. Intramolecular motions of a zinc finger DNA-binding domain from Xfin characterized by proton-detected natural abundance ^{13}C heteronuclear NMR spectroscopy. *J. Am. chem. Soc.* **113**, 4371–4380 (1991).
42. Kraulis, P. Molscript - a program to produce both detailed and schematic plots of protein structures. *J. appl. Crystallogr.* **24**, 946–950 (1991).